Mechanics and Mechanical Engineering
Vol. 22, No. 4 (2018) 1287–1299


https://doi.org/10.2478/mme-2018-0099

# An Analysis and Modeling of the Dynamic Stability of the Cutting Process Against Self-Excited Vibration

A. Motallebia
*Department of Mechanical Engineering, Khoy Branch*
*Islamic Azad University, Khoy, Iran*

A. Doniavi
*Department of mechanical Engineering*
*Urmia University,Urmia,Iran*
*e-mail: gow.1976@gmail.com*

Y. Sahebi
*Department of Mechanical Engineering, Khoy Branch*
*Islamic Azad University, Khoy, Iran*

Received (12 Ferbruary 2018)
Revised (14 June 2018)
Accepted (20 November 2018)

Chatter is a self-excited vibration which depends on several parameters such as the dynamic characteristics of the machine tool structure, the material of the work piece, the material removal rate, and the geometry of tools. Chatter has an undesirable effect on dimensional accuracy, smoothness of the work piece surface, and the lifetime of tools and the machine tool. Thus, it is useful to understand this phenomenon in order to improve the economic aspect of machining. In the present article, first the theoretical study and mathematical modeling of chatter in the cutting process were carried out, and then by performing modal testing on a milling machine and drawing chatter stability diagrams, we determined the stability regions of the machine tool operation and recognized that witch parameter has a most important effect on chatter.

*Keywords*: machine tool vibrations, chatter, stability, modeling.

## 1. Introduction

Chatter is a self-excited vibration which occurs if the chip width is too large with respect to the dynamic stiffness of the system. Variable forces generated during the machining operation leads to vibrational excitation of the tools and workpiece and as a result, the surface of the workpiece becomes wavy. In the next machining stage, if the generated wavy surface is not in phase with the wavy surface of the previous stage, the thickness of the chip becomes variable and it will lead to a change in

the shear force. The change in the shear force will change the energy entering the system – including tools and workpiece.

And if the system does not have the capacity for the extra energy input, it will start vibrating which is referred to as chatter. Chatter vibration has an exponential growth in amplitude over time, and this continues until the tool is separated from the workpiece or that it breaks. This phenomenon can be distinguished by its sound or its marks on the workpiece surface.

Machining with chatter is in most cases an unwanted phenomenon, since it has an adverse effect on the surface of the workpiece and besides, it may break the tools or other parts of the machine tool. Therefore, the cutting width and material removal rate must be below the limit at which chatter occurs. From this perspective, chatter is a factor decreasing material removal rate before it is limited by the power and moment of the machine tool.

The simplest theory for calculating the cutting force which has been used in studying the stability of machining processes was founded by Tlusty [11]. Rao et al. [2] presented a cutting force model of oblique turning process and used it for drawing chatter stability diagrams. Baker and Rouch [3] used a finite element model for analyzing the stability of the turning process. In references [4–7] the effect of tool wear parameter on chatter has been examined. Tang [5] controlled chatter in the turning process by placing piezoelectric actuators on the tool. Liao [6] controlled chatter using a system for automatic spindle speed regulation. Pan et al. [7–12] developed an intelligent system for controlling chatter in the turning process using neural networks.

The width of the chip is the most important factor which plays a crucial role in generating chatter vibration. If chip width is small enough, machining will be stable. With the increase of material removal width, chatter starts at a $b$ limit and will be very severe for chip widths larger than this. The critical chip width depends on some factors such as the dynamic characteristics of the machine tool structure, the material of the workpiece, material removal rate, and the geometry of tools [8]. A negative cutting angle will increase the possibility of chatter, since the direction of cutting force with the negative cutting angle of tools will be mostly along the direction of vibration. The effect of the relief angle of the tool on the occurrence of chatter is displayed in the figure. Since the tool moves on a wavy surface, the relief angle (the angle in the above figure) is always changing and in location B where the relief angle is negative, much energy is lost from the system due to the contact between the tool and the workpiece. This phenomenon has been discussed as process damping [13] and is more noticeable at lower cutting speeds, since at higher cutting speeds the wavelength of oscillations increases and assuming the constancy of the vibration amplitude, the slope of the oscillations decreases and thus there will be less change in the relief angle [8–15].

## 2. Results and Discussion

### 2.1. *Modeling a Fixed-Hinged Beam with Cutting Tool in the Middle of the Beam*

The work piece studied in this article is a fixed-hinged beam; thus considering the new conditions, a support is obtained for the beam using the following equations:

$$\begin{aligned}
\frac{\partial u_2}{\partial x} &= \frac{T}{GJ}U_3 + \theta_3 \\
\frac{\partial u_3}{\partial x} &= \frac{-T}{GJ}U_2 - \theta_2 \\
\frac{\partial \theta_2}{\partial x} &= \frac{M_2}{EI_{22}} + \frac{T}{GJ}\theta_3 \\
\frac{\partial \theta_3}{\partial x} &= \frac{M_3}{EI_{33}} - \frac{T}{GJ}\theta_2 \\
\frac{\partial M_2}{\partial X} &= J_{22}\frac{\partial^2 \theta_2}{\partial t^2} - \left[\frac{T}{EI_{33}} - \frac{T}{GJ}\right] M_3 + V_3 \\
\frac{\partial M_3}{\partial X} &= J_{33}\frac{\partial^2 \theta_3}{\partial t^2} - \left[\frac{T}{EI_{22}} - \frac{T}{GJ}\right] M_2 - V_2 \\
\frac{\partial V_2}{\partial X} &= n_0\frac{\partial^2 U_2}{\partial t^2} - \frac{PM_3}{EI_{33}} + \frac{T}{GJ}V_3 - F_1 \\
\frac{\partial V_3}{\partial X} &= n_0\frac{\partial^2 U_3}{\partial t^2} + \frac{PM_2}{EI_{22}} - \frac{T}{GJ}V_2 - F_2
\end{aligned} \tag{1}$$

where $\theta_2$ and $\theta_3$ are the rotations of the beam in the 2 and 3 directions, $U_2$ and $U_3$ are displacements of the beam in the 2 and 3 directions, $M_2$ and $M_3$ are the bending moments in these two directions, $V_2$ and $V_3$ are the shear forces in these two directions novel method based on CEEM method to model five-axis cutting force.

## 3. Solving the Equations Governing the Beam

The studied beam is a steel beam with 1m length and 1cm×2cm rectangular cross-section. We take the vector of unknowns as

$$\begin{bmatrix} U_2 & U_3 & \theta_2 & \theta_3 & M_2 & M_3 & V_2 & V_3 \end{bmatrix}$$

and use the method of separation of variables in order to solve the equations. That is:

$$z\,(x,t) = z(x)e^{i\omega\tau} \tag{2}$$

The dynamic equations of the system consisting of 8 equations varying with time and space are solved using the method of separation of variables with respect to time and space. The dynamic effect of the temporal term appears in these equations in the form of a frequency term. By eliminating the temporal dependence from dynamic equations governing the behavior of the system, we arrive at 8 spatial equations for positions along the beam which can be solved by applying boundary constraints (conditions) with respect to space which are given in Fig. 4.2(a).

The solution method involves dividing the length of the beam into equal parts. For any $i$-th point along the beam a corresponding vector is defined as follows:

$$Z = \begin{bmatrix} U_2 & U_3 & \theta_2 & \theta_3 & M_2 & M_3 & V_2 & V_3 \end{bmatrix}^T \tag{3}$$

The spatial equations governing the behavior of the system are rewritten as a function in the form of a matrix. In the numerical solution, the Runge Kutta method is responsible for predicting the vector of unknowns and the Adams-Moulton method is responsible for correcting these predictions and of course solving the vector of the unknowns of all the points on the beam. The matrix form of the 8 dynamic equations is as follows [9]:

$$\frac{dz}{dx} = \tag{4}$$

$$\begin{bmatrix} 0 & \frac{T}{GJ} & 0 & 1 & 0 & 0 & 0 & 0 \\ \frac{-T}{GJ} & -1 & 0 & 0 & 0 & 0 & 0 & 0 \\ 0 & 0 & 0 & \frac{T}{GJ} & \frac{1}{EI22} & 0 & 0 & 0 \\ 0 & 0 & \frac{-T}{GJ} & 0 & 0 & \frac{1}{EI33} & 0 & 0 \\ 0 & 0 & -J_{22}\omega^2 & 0 & 0 & \frac{T}{EI33} - \frac{T}{GJ} & 0 & 1 \\ 0 & 0 & 0 & -J_{33}\omega^2 & \frac{T}{EI33} - \frac{T}{GJ} & 0 & -1 & 0 \\ -n_0\omega^2 & 0 & 0 & 0 & 0 & \frac{-P}{EI33} & 0 & \frac{T}{GJ} \\ 0 & -n_0\omega^2 & 0 & 0 & \frac{P}{EI22} & 0 & \frac{-T}{GJ} & 0 \end{bmatrix} \begin{bmatrix} U_2 \\ U_3 \\ \theta_2 \\ \theta_3 \\ M_2 \\ M_3 \\ V_2 \\ V_2 \end{bmatrix}$$

For any point, the vector $Z_i = C_1 {Z_i}^1 + C_2 {Z_i}^2 + \ldots C_8 {Z_i}^8$ corresponds to the $i$-th solution of the governing differential equation, In other words, $Z$ is of the form $z = [k]C$. At the beam, considering the physical constraints governing it, is as follows:

$$Z_1 = \begin{bmatrix} 0 \\ 0 \\ 0 \\ 0 \\ M_2 \\ M_3 \\ V_2 \\ V_2 \end{bmatrix} = C_1 \begin{bmatrix} 0 \\ 0 \\ 0 \\ 0 \\ 0 \\ 0 \\ 0 \\ 0 \end{bmatrix} + C_2 \begin{bmatrix} 0 \\ 0 \\ 0 \\ 0 \\ 0 \\ 0 \\ 0 \\ 0 \end{bmatrix} + \cdots + C_8 \begin{bmatrix} 0 \\ 0 \\ 0 \\ 0 \\ 0 \\ 0 \\ 0 \\ 1 \end{bmatrix} \tag{5}$$

The first four coefficients of the solution model are equal to zero:

$$C_1 = C_2 = C_3 = C_4 = 0 \tag{6}$$

Using the superposition method and by applying eight boundary conditions at the tip of the beam and integrating for each of these conditions along the beam using a predictor-corrector algorithm, the $K$ matrix is obtained at the end of the beam. By applying the boundary conditions at the end of the beam as given below,

$$Z = \begin{bmatrix} K_{11} & K_{11} & . & . & . & K_{18} \\ K_{21} & K_{22} & . & . & . & K_{28} \\ \vdots & & & & & \\ K_{81} & K_{82} & . & . & . & K_{88} \end{bmatrix} \begin{bmatrix} 0 \\ 0 \\ 0 \\ 0 \\ C_5 \\ C_6 \\ C_7 \\ C_8 \end{bmatrix} = \begin{bmatrix} 0 \\ 0 \\ \theta_2 \\ \theta_3 \\ 0 \\ 0 \\ V_2 \\ V_3 \end{bmatrix} \tag{7}$$

we arrive at the following equations:

$$\begin{aligned} k_{15}C_5 + k_{16}C_6 + k_{17}C_7 + k_{18}C_8 &= 0 \\ k_{25}C_5 + k_{26}C_6 + k_{27}C_7 + k_{28}C_8 &= 0 \\ k_{35}C_5 + k_{36}C_6 + k_{37}C_7 + k_{38}C_8 &= 0 \\ k_{65}C_5 + k_{66}C_6 + k_{67}C_7 + k_{68}C_8 &= 0 \end{aligned} \tag{8}$$

The condition for the above homogeneous system (of the form $K[C] = 0$) to have a solution is that the determinant of matrix $[K]$ equals zero. The result of this condition implies that $\det[K] = 0$ is a function of $\omega$. The natural frequencies of the model are obtained by numerically solving these equations. The figure below displays the diagram of changes that has been estimated at the points where this function meets the horizontal axis, and of course these frequencies are the natural frequencies of the system.

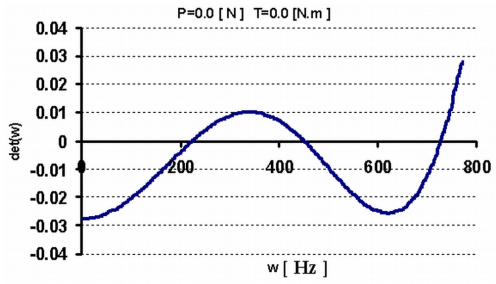


**Figure 1** $\det(w)$ vs. $w$

The following diagram shows the variation of the first frequency of the beam with the load applied at the end of the beam. According to the figure, the point where frequency reaches zero corresponds to the critical force for the buckling phenomenon. In the proposed model, the load applied at the end of the beam is the same as the load generated by the mandrel.

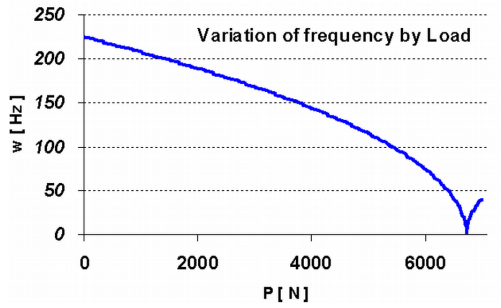


**Figure 2** The natural frequency of the system in $p$ (power) for finding

After numerical solution of the system, four natural frequencies are obtained and ultimately the mode shapes related to each of these frequencies are drawn which, correspond to beam displacement and beam and bending.

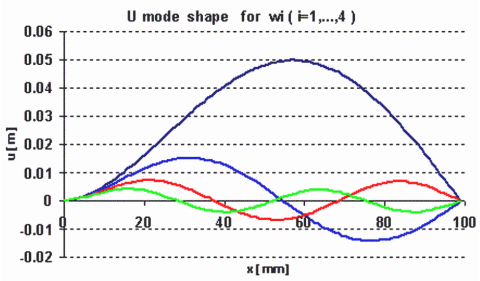


**Figure 3** Mode shapes and (displacements in the 2 and 3 directions)

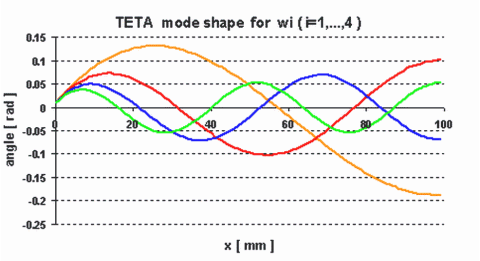


**Figure 4** Mode shapes related to rotations $\theta_2$ and $\theta_3$

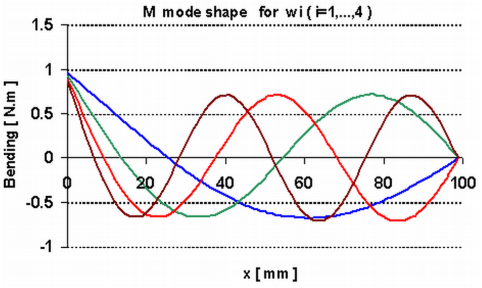


**Figure 5** Mode shapes related to bending moments $M_2$ and $M_3$

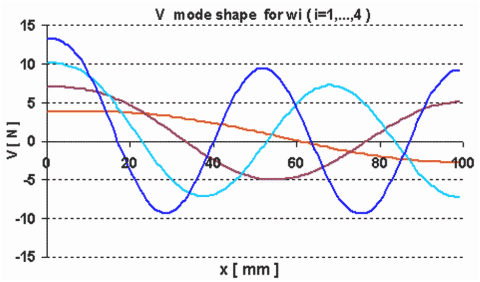


**Figure 6** Mode shapes related to shear forces $V_2$ and $V_3$

### 3.1. *The Dynamic Equations Governing the Behavior of the Cylindrical Work piece*

In the next stage of system simulation, a cylindrical work piece with length and radius has been used instead of a work piece with a rectangular cross-section, and in this situation the equations governing the dynamic behavior of the system are simplified as follows:

$$\begin{aligned} \frac{\partial U}{\partial X} - \theta &= 0 \\ \frac{\partial \theta}{\partial X} - \frac{M}{EI} &= 0 \\ J\frac{\partial^2 \theta}{\partial t^2} - \frac{\partial M}{\partial X} + V &= 0 \\ n_0 \frac{\partial^2 \theta}{\partial t^2} - \frac{P}{EI}.M - \frac{\partial V}{\partial X} &= F \end{aligned} \tag{9}$$

By arranging the equations governing the cylindrical beam under the load we have:

$$\begin{aligned} Z = \begin{bmatrix} n_0 & 0 & 0 & 0 \\ 0 & -J & 0 & 0 \\ 0 & 0 & 0 & 0 \\ 0 & 0 & 0 & 0 \end{bmatrix} \begin{bmatrix} \frac{\vartheta^2 U}{\vartheta^2} \\ \frac{\vartheta^2 \theta}{\vartheta^2} \\ \frac{\vartheta^2 M}{\vartheta^2} \\ \frac{\vartheta^2 V}{\vartheta^2} \end{bmatrix} + \begin{bmatrix} 0 & 0 & 0 & +1 \\ 0 & 0 & +1 & 0 \\ 0 & +1 & 0 & 0 \\ +1 & 0 & 0 & 0 \end{bmatrix} \begin{bmatrix} \frac{\vartheta U}{\vartheta X} \\ \frac{\vartheta \theta}{\vartheta X} \\ \frac{\vartheta M}{\vartheta X} \\ \frac{\vartheta V}{\vartheta X} \end{bmatrix} \\ + \begin{bmatrix} 0 & 0 & +\frac{P}{EI} & 0 \\ 0 & 0 & 0 & -1 \\ 0 & 0 & \frac{-1}{EI} & 0 \\ 0 & -1 & 0 & 0 \end{bmatrix} \begin{bmatrix} U \\ \theta \\ M \\ V \end{bmatrix} = \begin{bmatrix} F \\ 0 \\ 0 \\ 0 \end{bmatrix} \end{aligned} \tag{10}$$

Or in the general form of

$$A_1 \frac{\partial^2 Z}{\partial t^2} - \frac{\partial Z}{\partial X} + A_2 Z = b. \tag{11}$$

$$\tilde{z}(t,x) = \int_{j=1}^{n} f_j(t) Z_0^{(j)}(x) \tag{12}$$

Considering the generalized principle of virtual work, we have

$$\int_0^1 \left[ L(\tilde{z}) E_0 {Z_0}^{(i)} \right] dx = 0 \tag{13}$$

And in the above relation

$$L\left(Z\right) = A_1 \frac{\partial^2 Z}{\partial t^2} + A_2 \frac{\partial Z}{\partial t} - \frac{\partial Z}{\partial X} A_3 Z = b \tag{14}$$

Finally, by simplifying and integrating the above relations we come to the following relation:

$$\int_{j=1}^{k} a_{ij} \frac{d^2 f_j}{d\tau^2} + b_{ij} \frac{df_j}{d\tau} + c_{ij} f_j = d_{ij} \varphi_j \ , \ i,j = 1 \ldots k \tag{15}$$

Where the number of vibrational modes is used which are obtained by solving the free vibration of the system corresponding to each of the displacements, rotations, moments, and shear forces. The vector form of the equation is as:

$$A\frac{d^2f}{d\tau^2} + B\frac{df}{dt} + Cf = D\Delta T \tag{16}$$

So that in the above relations we have:

$$A = [a_{ij}], \quad B = [b_{ij}], \quad C = [c_{ij}], \quad D = [d_{ij}] \tag{17}$$

$$\begin{aligned} a_{ij} &= \int_0^1 \{A_1 {Z_0}^{(j)} E_0 {Z_0}^{(i)}\} dx \\ c_{ij} &= \int_0^1 A_3 {Z_0}^{(j)} - \frac{d{Z_0}^{(j)}}{d\mathrm{X}} E_0 {Z_0}^{(i)} dx \end{aligned} \tag{18}$$

By providing a computer code for solving the system using the algorithm presented above, and are obtained which correspond to the mass and fitness of the system. Considering the way of aligning the tool relative to the workpiece, we expect the first mode shape of the beam to be excited and the effect of the following mode shapes to be insignificant in comparison with the effect of the first frequency. Thus, by eliminating the effect of higher frequencies, we can assume the model of the workpiece as a system with one degree of freedom. Considering the fact that the value of for the first frequency is equivalent to the mass of the system with one degree of freedom and the value of is equivalent to the stiffness of the system with one degree of freedom, we can assume that the system has a damping coefficient. In this model, the damping coefficient for the cutting dynamics has been empirically obtained; thus, our workpiece model is a simple mass-spring-damper model. It must be noted that since the piece is cut at the middle, the first frequency is excited and the subsequent effects are eliminated.

## 4. Mechanisms of Chatter Phenomenon in Machining

Self-excited vibrations in machine tools are due to two fundamental mechanisms, mode coupling and regeneration of waviness, and in this section we will explain these mechanisms.

### 4.1. *Mode Coupling Effect*

Self-excited vibrations due to mode coupling occur when there are vibrations between the tool and the workpiece at the same time and in two different directions. As can be seen in the figure, the tool and its support are modeled as a concentrated mass, $m_1$, and two springs, $Ak_1$ and $k_{21}$, orthogonal to one another. If we assume that the movement of the workpiece is from right to left and the tool is fixed, clearly the shear force will lead to vibrational motion in two orthogonal directions with different amplitudes, and as a result the tool tip will move in an elliptical path. Now, taking into consideration the shape and direction of the tool tip inside the workpiece, for a part of the path where the tool tip travels the distance from A to B (considering the direction of the shear force), the direction of the force is opposite to the displacement and it will lead to energy loss. In the second part of the path for the cycle to become complete, the tool tip travels the distance from B to A. In this part of the path, the direction of the shear force and the displacement of the

tool tip are the same which will cause energy to transfer from the workpiece to the tool. Since the cutting depth in the B to A path is larger than the A to B path and considering the approximate equality of the two paths, the energy transferred to the tool is greater than the energy lost from it. This surplus of energy of the tool will sustain its vibrations against damping losses and as a result the tool will continue its vibrations [11, 14].

### 4.2. *Waviness Regeneration*

In machining operations, machining is done on a surface that has already been produced by the tool in the previous pass. This surface has been produced by the previous tooth in the milling operation and by the previous revolution in the turning operation. If for any reason (e.g., bending vibrations of the workpiece due to the cutting force) a relative oscillation is produced between the tool and the workpiece, the tool tip will encounter a wavy surface in the next pass (the next revolution in the turning operation and the next tooth in the milling operation) and consequently it will lead to an alternating change in chip thickness and the result will be the alternating change of the machining force. This alternating cutting force will intensify vibrations and their amplitude will vary depending on the machining conditions. Thus, the newly generated surfaces will also be wavy. Accordingly, the generation of wavy surfaces will ceaselessly continue and the phase difference between wavy surfaces in two consecutive passes will be constrained by the geometry of the machining operation; this phase difference in turn affects the regeneration of wavy surfaces (Fig. 4).

In the turning operation, the phase difference between two consecutive waves can be denoted by the relationship between the revolution speed of the spindle $n$ and vibration frequency $N + \frac{\epsilon}{2\pi} - \frac{f}{n}$ where $N$ is the maximum number of full waves on the workpiece so that $\frac{\epsilon}{2\pi} < 1$. In other words, full waves and a part of a full wave $(\frac{\epsilon}{2\pi})$ are produced on the workpiece surface. As can be seen in th figure, depending on the value of, chip thickness variation $(Y_0 - Y)$ can be either equal to zero (if $\epsilon$ is zero) or a maximum value. Clearly, if $\epsilon$ is zero, there will be no chatter, since the wavy surfaces in two consecutive passes will be parallel and consequently there will be no change in the cutting force which is due to chip thickness variation.

### 4.3. *Analysis of the Chatter in Turning Process*

Assume that in turning process, the tool is machining in the direction orthogonal to the workpiece axis. The bending vibrations of the workpiece due to the cutting force will generate a wavy surface on its cross-section. If the workpiece is modeled using a model with one degree of freedom as specified in Fig. 5, the vibration equation of the system will be of the form of relation (1):

$$m_y \ddot{y}(t) + c_y \dot{y}(t) + k_y y(t) = F(t) \tag{19}$$

The machining force $F(t)$ can be calculated from the following relation:

$$F(t) = k_f a h(t) \tag{20}$$

where $K_f$ is the shear strength and is the chip width; is the dynamic (instantaneous) thickness of the chip expressed by the nominal thickness of the chip ($h_0$) and vibration function on the machining surface in the current machining pass, $y(t)$, and the previous machining pass, $y(T-t)$ is the rotation period of the spindle.

$$h\left(t\right) = h_0 + y\left(t-T\right) - y(t) \tag{21}$$

Thus, the machining force depends on the relative vibration between the tool and the workpiece in the current and previous pass combining the relations will yield a delay differential equation in the temporal domain:

$$m\ddot{y} + c\dot{y} + ky = k_f a[h_0 + y\left(t-T\right) - y\left(t\right)] \tag{22}$$

The above equation is expressed in the Laplace domain as follows:

$$\left[ms^2 + cs + k\right] y\left(s\right) = k\ a[h_0 + \left(e^{-sT} - 1\right) y\left(s\right)] \tag{23}$$

On the other hand,

$$y\left(s\right) = F(s)\phi(s) = k_f a h(s)\phi h(s) \tag{24}$$

where $\varphi(s)$ is the transformation function of the relative vibration of the tool and the workpiece. Combination of the above relations gives:

$$h\left(s\right) = h_0 + (e^{-sT} - 1)k_f a h(s)\phi h(s) \tag{25}$$

Thus, characteristic equation of chatter vibrations is expressed as:

$$\frac{Hs}{H0} - \frac{1}{(\vartheta^{-sT} - 1)\ h_f a\varphi s} \tag{26}$$

In other words, the above equation is the transformation function between the nominal and instantaneous thickness. The stability of chatter vibrations is represented as a control diagram; nominal thickness $h_0$, system input, and system output are a function of instantaneous vibrations $y(t)$. The stability of the system against self-excited vibrations will be equivalent to the stability of the above closed-loop control diagram. The stability of a closed-loop system is determined by the roots of the characteristic equation and if the real component of the root of the characteristic equation is negative in the Laplacian domain, the system will be stable. The root of the characteristic equation is in the stability boundary of the system, where is the angular chatter frequency. Thus,

$$1 + \left(1 - e^{-j\omega_c T}\right) k_f a\varphi\ \varphi\left(j_c\right) = 0 \tag{27}$$

If the real and imaginary parts of the transformation function of system vibration be as

$$\varphi\left(j\omega_c\right) = G\left(\omega_c\right) + jH(\omega_c) \tag{28}$$

Since

$$e^{-j\omega_c T} = \cos\left(\omega_c T\right) - j\sin(\omega_c T) \tag{29}$$

The combination of the above relations gives:

$$\{1 + k_j a[G(\omega_c)(1 - \cos(\omega_c T)) - H(\omega_c)\sin(\omega_c T)]\} + j\{k_f a[G(\omega_c)\sin(\omega_c T) + H(\omega_c)(1 - \cos(\omega_c T))]\} = 0 \quad (30)$$

which will be obtained from the latter relation of the system of equations.

$$G(\omega_c)\sin(\omega_c T) + H(\omega_c)(1 - \cos(\omega_c T)) = 0 \quad (31)$$

and

$$1 + k_f a[G(\omega_c)(1 - \cos(\omega_c T))] - H(\omega_c)\sin(\omega_c T) = 0 \quad (32)$$

In the above relations, chip width ( a ) is a parameter that depends on the machining process. Thus, the goal is to determine the chip width values that put the system at the stability boundary.

If is the phase angle of the transformation function of the system at the stability boundary, then,

$$\tan \Psi = H(\omega_c)/G(\omega_c) \quad (33)$$

And finally we come to the following relation:

$$a_{lim} = \frac{-1}{2k_f G(\omega_c)} \quad (34)$$

The above relation indicates the maximum cutting width which can exist without chatter vibrations. Since cutting width is a quantity whose negative value has no physical meaning, the above equation only holds for the negative values of the real part of the transformation function. This equation expresses that the critical cutting width has an inverse relationship with the flexibility if the machine tool; the more flexible the structure and the greater the cutting strength are, the lower will be the critical cutting width value and chatter vibrations will start at lower values of cutting width.

## 5. Analysis and Dynamic Modeling of Cutting

In the present paper, the dynamic model of the studied machining system is as below, where the dynamics governing cutting are described by the Mathieu equation and this behavior of the equation has been modeled using the Simulink extension of the Matlab Software.

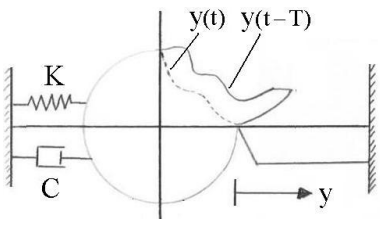


**Figure 7** The dynamic model of the machining system

$$I = \int_0^t \frac{\pi d}{60} \left(n_0 t + \Delta n \sin \omega_N t\right) dt = \frac{\pi D}{60} (n_0 + \Delta n \sin(\omega N^t))^{\,2} \tag{35}$$

$$c(1) = \frac{\pi D_m \Delta n \omega_n}{60} \cos\left(\omega N^t\right) + \frac{\pi D_c}{60} \left(n_0 + \Delta n \sin(\omega N^t)\right) \tag{36}$$

$$k(1) = k\,, \quad b_1(1) = -c_3(t)(b_0 + c_1)\cos\theta \tag{37}$$

$$c_1 = a_0 \cot(k_\gamma + k'_\gamma) + \tan\theta \quad c_3 = \frac{2\tau_S \sin(\beta - \gamma)}{\cot(\beta - \gamma) - \sin(\beta - \gamma)} \tag{38}$$

Finally, we obtain:

$$my''(t) + cy'(t) + ky(t) = -c_3(t)\cos\theta\,((b_0 + c_1)y(t)) \tag{39}$$

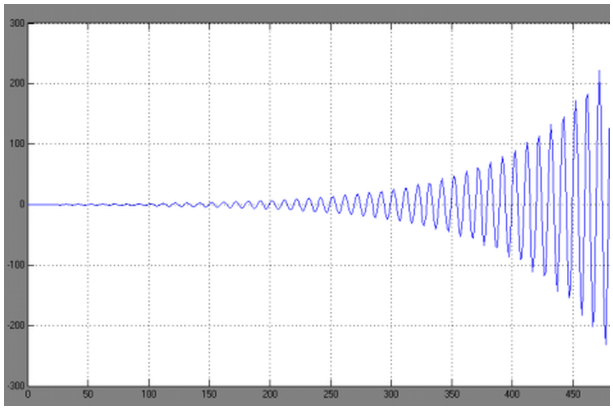


**Figure 8** Amplitude versus time for $n_0 = 850$, $y = -8$ and $b = 0.2$ (towards stability)

In order to examine the effects of the parameters $y'$ and $h_0$, on the chatter phenomenon, different pairs of effective parameters have been simulated and some of them are presented in Figs. 8 and 9.

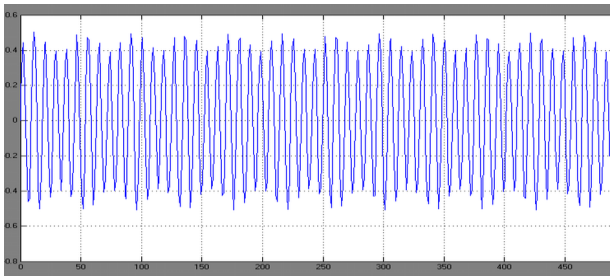


**Figure 9** Amplitude versus time for $n_0 = 325$, $y = -8$ and $b = 0.2$ (stability state)

## 6. Conclusion

In obtaining the natural frequencies of a system, if the load (the force exerted on the cylindrical workpiece due to closing the mandrel) is exerted on the workpiece, the natural frequency of the system ($\omega$) will decrease due to the reduction of beam stiffness. If we draw the diagram of (mandrel force) in (natural frequency), the critical point for the force will be: $P_{cr} = 6730\,\mathrm{N}$.

## References


[1] **Tlusty, G. and Polacek, M.**: *The stability of machine tools against self-excited vibrations in machining*, in: Proceedings of the ASME International Research in Production Engineering, Pittsburgh, USA, 465–474, **1963**.

[2] **Rao, B. and Shin, Y.C.**: A Comprehensive Dynamic Cutting Force Model for Chatter Prediction in Turning, *International Journal of Machine Tools and Manufacture*, **39**, 1631–1654, **1999**.

[3] **Baker, J.R. and Rouch, K.E.**: Use of Finite Element Structural Models in Analyzing Machine Tool Chatter, *Finite Elements in Analysis and Design*, **38**(11), 1029–1046, **2002**.

[4] **Chiou, Y.S. and Liang, S.Y.**: Chatter Stability of a Slender Cutting Tool in Turning with Tool Wear Effect, *International Journal of Machine Tools and Manufacture*, **38**(4), 315–327, **1998**.

[5] **Tang, Y.S., Kao, J.Y. and Lee, E.C.**: Chatter suppression in turning operations with a tuned vibration absorber, *Journal of Materials Processing Technology*, **105**, **2000**.

[6] **Chen, M.**:. *Self-induced chatter vibration of lathe tools*, **1972**.

[7] **Galewski, M. and Kalinski, K.**: *Vibration surveillance during high speed milling with variable spindle speed*, The Publication of Gdansk University of Technology (in Polish), Gdansk, **2009**.

[8] **Schmitz, T.L., Burns, T.J., Ziegerta, J.C., Duttererc, B. and Winfough, W.R.**: Tool Length-Dependent Stability Surfaces, *Machining Science and Technology*, **8**(3), 377–397, **2004**.

[9] **Yosuke, M., Takashi, M. and Eiji, U.**: Simulation Analysis of Self-Excited Chatter Vibration with Taking the Non-Linearity of Machine-Tool Structure into Account, 3rd Report, *Journal of the Japan Society for Precision Engineering*, **2008**.

[10] **Altintas, Y.**: *Manufacturing Automation. Metal Cutting Mechanics, Machine Tool, Vibrations and CNC Design*, Cambridge University Press, **2009**.

[11] **Tlusty, G.**: *Manufacturing processes and Equipment*, **2000**.

[12] **Ulf J., Aarsnes, F., Morten Aamo, O.**: Linear stability analysis of self-excited vibrations in drilling using an infinite dimensional model, *Journal of Sound and Vibration*, **360**, 239–259, **2016**.

[13] **Anindya, M., Chatterjee, S.**: Modal self-excitation by nonlinear acceleration feedback in a class of mechanical systems, *Journal of Sound and Vibration*, **376**, 1–17, **2016**.

[14] **Sunb, C., Altintasa, Y.**: Chatter free tool orientations in 5-axis ball-end milling, *International Journal of Machine Tools and Manufacture*, **106**, 89–97, **2016**.

[15] **Erdbrink, D.E., Krzhizhanovskaya, V.V.**: Differential evolution for system identification of self-excited vibrations, *Journal of Computational Science*, **10**, 360–369, **2016**.